Macromolecules

pubs.acs.org/Macromolecules Article

Photoreversible Order−Disorder Transitions in Block Copolymer/Ionic Liquid Solutions

Claire L. Seitzinger, Cecilia C. Hall, and Timothy P. Lodge*

Cite This: https://doi.org/10.1021/acs.macromol.2c00397 Read Online

ACCESS | Metrics & More | Article Recommendations | Supporting Information

ABSTRACT: External stimuli are of interest in controlling the nanoscale morphology in self-assembling polymer materials. While temperature is commonly used to control the state of microphase separation in block polymer solutions, light is a highly tunable, contactless method that can be spatially selective. Here, we use UV irradiation to induce order−disorder transitions (ODTs) in concentrated solutions of four poly(methyl methacrylate)-*b*-poly(benzyl methacrylate-*s*-4-phenylazophenyl methacrylate) block copolymers in three imidazolium-based ionic liquids. Due to a significant change in polarity in the phenylazophenyl methacrylate monomer upon UV irradiation, a bistable temperature window exists between the ODT in the dark and under UV irradiation, allowing for light-triggered ODTs. UV-irradiated small-amplitude oscillatory shear rheology is used to locate the bistable window and then to trigger ODTs reversibly with light. The ordered states formed in the dark are determined by small-angle X-ray scattering. Three tunable factors are explored within the system: the relative lengths of the copolymer blocks, the selectivity of the solvent, and the content of the photoactive monomer. The block composition was found to mainly influence the ordered state formed by the system after microphase separation. The selectivity of the solvent is the most promising method for tuning the ODT temperature, and the amount of photoactive monomer controls the width of the bistable window.

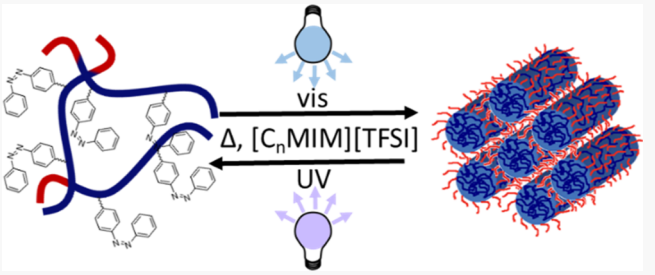

INTRODUCTION

Control over nanoscale morphology in block polymers has been an important aspect of technological development from selective patterning of microchips to separation membranes with improved transport properties.[1−10] Additionally, the ability to reverse such patterning and switch between morphologies could expand applications, for example in drug delivery and repositionable adhesives.[11−13] Numerous stimulus-responsive systems have been developed; common stimuli include heat, pH, and light.[14−16] Thermo-responsive behavior is the most well-studied, but not all applications are amenable to changes in the temperature. Light allows for a contactless stimulus with both excellent temporal and spatial resolution. In this study, we combine temperature and light stimuli to explore an alternative method of controlling phase behavior in block polymers.

Block polymers in concentrated solutions and melts display two major classes of thermo-responsive phase behavior: upper and lower critical ordering transitions (UCOT and LCOT), depending on the sign of the correlation between temperature and the segregation strength.[17−23] A UCOT polymer solution transitions from order to disorder upon heating, whereas microphase separation occurs upon heating for LCOT solutions. An LCOT arises when one of the blocks exhibits lower critical solution temperature (LCST) behavior (liquid−liquid phase separation upon heating) as a homopolymer in the solvent of interest. In diblock copolymers, generally the solvent is chosen to be a good solvent for the other block. Some well-studied LCST examples include poly(*N*-isopropyl acrylamide) in water,[24−26] poly(*n*-butyl methacrylate) in the ionic liquid 1-ethyl-3-methyl imidazolium bis(trifluoromethylsulfonyl)imide ([C_2MIM][TFSI]),[27,28] and poly(benzyl methacrylate) (PBnMA) in [C_2MIM][TFSI].[15,29−33] In [C_2MIM][TFSI], a suitable neutral block is poly(methyl methacrylate), as it is completely soluble over a wide temperature window.[38]

Here, a diblock copolymer solution is presented that responds to both thermo- and photo-stimuli. Previous research has incorporated photoactive monomers into existing thermo-responsive polymer solutions.[34−37,39−41] Ueki *et al.* discovered that by incorporating just 2 mol % of an azobenzene-based monomer into PBnMA, there was a 15 °C window between the phase separation temperatures of [C_2MIM][TFSI] in the dark (90 °C) and under UV irradiation (105 °C).[34] This allowed phase separation to be controlled by a light stimulus between the two temperatures. Azobenzene is an advantageous photo-trigger for polymer solutions. It undergoes *trans* to *cis*

Received: February 23, 2022
Revised: April 9, 2022

isomerization under UV irradiation (365 nm) that is readily reversible by irradiation with visible light.[42] Additionally, azobenzene does not exhibit significant decomposition pathways, leading to robust, long-lasting, light-responsive materials. The change in dipole moment is significant, from 0.53 D (*trans*) to 3.08 D (*cis*), which changes the solubility of the molecule substantially, with the *cis* form more soluble in polar solvents such as ionic liquids.[42,43] Recently, Hall and Lodge investigated the photoreversible phase behavior of poly(methyl methacrylate)-*block*-poly(benzyl methacrylate-*stat*-4-phenylazophenyl methacrylate) in $[C_2MIM][TFSI]$.[44] The system showed different order−disorder transitions (ODTs) in the dark *versus* under UV irradiation, and the authors demonstrated that there was a bistable temperature window in which the ODT could be triggered with light. Here, we build upon that work by exploring the effects of various parameters, including the block ratio, amount of azobenzene incorporated into the polymer, and choice of the ionic liquid.

MATERIALS AND METHODS

Experimental Section. *Materials.* 4-Cyano-4-[(dodecylsulfanylthiocarbonyl)sulfanyl]pentanoic acid, 4,4′-azobis(4-cyanovaleric acid), tris(2-carboxyethyl)phosphate hydrochloride, *n*-propyl amine, and methyl acrylate were used as purchased from Sigma-Aldrich. 4-Phenylazophenyl methacrylate (AzoMA) was synthesized from methacryloyl chloride and 4-phenylazophenol, as previously described.[45] Methyl methacrylate and benzyl methacrylate were purchased from Sigma-Aldrich, and inhibitors were removed by passing through a neutral alumina column. The ionic liquids $[C_2MIM][TFSI]$ and $[C_4MIM][TFSI]$ were synthesized as previously described *via* ion exchange in water.[46] $[C_1MIM][TFSI]$ was purchased from IoLiTec. All ionic liquids were purified *via* liquid−liquid extraction from water into dichloromethane (DCM) and then by stirring charcoal in the DCM solution, which was removed by filtration. The DCM was removed by rotary evaporation, and the ionic liquid was dried in a vacuum oven at 100 °C for three days. Ionic liquid purity was confirmed by ^{1}H NMR and ^{19}F NMR spectroscopy (see Supporting Information).

Polymer Synthesis. The block copolymers were synthesized by sequential RAFT polymerization as previously described, including removal of the chain transfer agent (CTA) after polymerization.[44] A representative synthesis is as follows: a dried Schlenk flask was charged with a stir bar, methyl methacrylate (20 g, 200 mmol) purified over neutral alumina, 4-cyano-4-[(dodecylsulfanylthiocarbonyl)sulfanyl]pentanoic acid (0.49 g, 1.2 mmol), and 4,4′-azobis(4-cyanovaleric acid) (0.034 g, 0.12 mmol) in dioxane (40 mL). The flask was degassed by three freeze−pump−thaw cycles under argon. The reaction was stirred at 80 °C for 7.5 h and was then quenched by opening the flask in the air and cooling on ice. The solution was diluted with DCM, precipitated into hexanes (10 times volume of solution), and vacuum filtered to recover the polymer. The polymer was precipitated into hexanes from a DCM solution twice more before drying at 100 °C under vacuum overnight. The poly(methyl methacrylate) (PMMA or M) macroinitiator was characterized by ^{1}H NMR spectroscopy and size exclusion chromatography (SEC, Figures S1 and S2), giving M_n = 16 kg/mol and $Đ$ = 1.06.

The purified PMMA (10 g, 0.53 mmol) was then added to a dried Schlenk flask along with benzyl methacrylate (31 g, 175 mmol) purified over neutral alumina, AzoMA (2.5 g, 9.0 mmol), and 4,4′-azobis(4-cyanovaleric acid) (0.0019 g, 0.0068 mmol) in dioxane (76 mL). The flask was degassed by three freeze−pump−thaw cycles under argon, and the reaction was allowed to run at 80 °C for 20 h. The reaction was quenched by opening the flask to air and cooling it on ice. The solution was diluted with DCM, precipitated into hexanes (10 times the volume of solution), and vacuum filtered to recover the polymer. The polymer was precipitated into hexanes from a DCM solution twice more before drying under vacuum overnight.

The CTA was cleaved from the final block copolymer *via* aminolysis and Michael addition with methyl acrylate. MBsA-CTA (31 g, 0.36 mmol) was dissolved in tetrahydrofuran (THF) (200 mL) in a round bottom flask, along with tris(2-carboxyethyl)phosphate hydrochloride (0.224 g, 0.78 mmol) dissolved in water (4 mL). The reaction flask was degassed with argon for 15 min. *N*-Propylamine (2.8 g, 47 mmol) was added, and the reaction was allowed to stir for 5 h. Methyl acrylate (8.55 g, 99 mmol) was added to the flask, and the mixture was allowed to stir for 12 h. The THF was removed by rotary evaporation, and the polymer was purified by precipitation three times, with DCM as the good solvent and hexane as the poor solvent.

Removal of the CTA was confirmed by ^{1}H NMR spectroscopy, with peaks characteristic of the CTA between 1 and 1.5 ppm unobserved after cleavage, and SEC (see Supporting Information, Figures S1, S4, and S6). CTA removal could not be quantified by UV/vis spectroscopy due to the overlap in absorbance between AzoMA and the CTA. The polymer was characterized by ^{1}H NMR spectroscopy and SEC (see Supporting Information); M_n = 49 kg/mol, $Đ$ = 1.04, n_{AzoMA} = 5 mol % in the BsA block, and f_{PMMA} = 0.2, assuming additivity of volumes and densities of 1.15 and 1.17 g/mL for the M and BsA blocks, respectively.[47]

Material Characterization. Proton nuclear magnetic resonance (^{1}H NMR) spectra of the polymers, the ionic liquids, and the AzoMA monomer were collected using a 400 MHz Bruker Avance III HD spectrometer, with deuterated DCM, deuterated dimethyl sulfoxide, and deuterated chloroform as solvents, respectively. Molar mass distributions for the polymers were obtained using SEC equipped with a refractive index (Wyatt Optilab rEX) and multi-angle light scattering detectors (Wyatt DAWN HELEOS II) with THF as the eluent. The dn/dc of the polymers in THF was calculated using a weighted average of the dn/dc values from M (0.086 mL/g),[48] B (0.144 mL/g),[49] and AzoMA (0.259 mL/g),[15] where the weight percent monomer in the polymer was calculated from the ^{1}H NMR spectra.[50] All ^{1}H NMR spectra and SEC traces can be found in the Supporting Information.

Solution Preparation. Samples were prepared at 35 wt % polymer *via* a cosolvent method. The polymer (0.35 g) and ionic liquid (0.65 g) were weighed into a 20 mL scintillation vial with a small stir bar. 10 mL of THF was added to the solution, which was allowed to stir for at least 2 h. The solution was filtered through a PTFE filter (13 mm, 0.45 μm). The THF was then removed by N_2 purge, followed by the vials being placed in a vacuum oven at 100 °C overnight. Samples were stored in a desiccator under vacuum.

Small Amplitude Oscillatory Shear Photo-rheology. Small-amplitude oscillatory shear (SAOS) was performed on a TA Instruments Discovery HR3 rheometer fitted with an electrically heated upper plate (40 mm dia.) and a quartz lower plate (20 mm dia.). An in-depth description of this set-up, including that of the UV lower plate attachment, was provided in previous work.[44] An Omnicure S1500 mercury arc lamp was used for irradiation, with 365 and 400−500 nm wavelength filters to allow for UV and visible wavelength penetration, respectively. Here, samples were measured with a gap of less than 300 μm. Temperature sweeps were performed from 30 to 150 °C at a frequency of 1 rad/s and a strain of 1%. Strain sweeps were performed at 30 and 150 °C to ensure that the measurements were taken in the linear viscoelastic regime. Frequency sweeps were also performed at various temperatures after the initial temperature sweeps, with annealing at 100 °C for 30 min prior to measurements in the dark (no irradiation and a shield in place) and annealing at 30 °C under UV radiation for 30 min prior to measurements under UV illumination with the same shield in place. For all cases, the ODT is taken as the point where the storage modulus, G', is equal to the loss modulus, G'', or where $\tan(\delta) = G''/G' = 1$; $\tan(\delta) > 1$ indicates a disordered sample and $\tan(\delta) < 1$ an ordered state.

Small-Angle X-ray Scattering. Small-angle X-ray scattering (SAXS) was performed at Sector 5-ID-D of the Advanced Photon Source at Argonne National Laboratory. The samples were loaded

https://doi.org/10.1021/acs.macromol.2c00397
Macromolecules XXXX, XXX, XXX−XXX

into aluminum sample pans and then dried in a vacuum oven at 100 °C overnight prior to loading into a glovebox and sealed hermetically. Measurements were taken upon heating from 30 to 175 °C with about 10 min of annealing at each temperature. The sample-to-detector distance was fixed at 7.5 m, the beam energy was 17.5 keV (wavelength λ = 0.7293 Å), and SAXS data were collected using a Rayonix area detector. The isotropic 2D data were reduced by azimuthal integration to give intensity as a function of the scattering wave vector, q. SAXS measurements were taken in the dark.

RESULTS

A total of four poly(methyl methacrylate)-*b*-poly(benzyl methacrylate-*s*-4-phenylazophenyl methacrylate) (MBsA) materials were synthesized: two symmetric and two asymmetric block copolymers, where the volume fraction of the stimulus-responsive block was increased to 80 vol %. Both pairs of copolymers were prepared with either 5 or 12 mol % AzoMA incorporation to explore how adding more photoactive monomer impacts the ODT window. The synthesized polymers are listed in Table 1. The nomenclature for the

Table 1. Polymer Characteristics

Sample	M_n [a] (kg/mol)	M_w [a] (kg/mol)	$Đ$	f_{PMMA} [b]	n_{AzoMA} [b] (mol %)
s-MBsA$_5$	65	66	1.01	0.5	5
a-MBsA$_5$	49	51	1.04	0.2	5
s-MBsA$_{12}$	62	67	1.08	0.5	12
a-MBsA$_{11}$	68	75	1.09	0.3	11

[a]Determined *via* SEC-MALS. [b]Determined *via* ^{1}H NMR spectroscopy.

polymers is as follows: s-MBsA$_n$, where s- indicates that the block copolymer is symmetric (for asymmetric a- is used) and n is the mol % incorporation of AzoMA, indicated as A, in the poly(benzyl methacrylate) (B) block.

To locate the ODT ($G' = G''$) as a function of temperature, all polymers were studied at a representative concentration of 35 wt % by SAOS rheology. Additionally, SAXS data were collected for the samples in the dark (*trans*-AzoMA) to corroborate the SAOS rheology results.

Effect of the Photoresponsive Block Volume Fraction. To explore the effect of composition on the ODT, the photoresponsive behavior of a-MBsA$_5$ in [C$_2$MIM][TFSI] was compared to that of s-MBsA$_5$ in the same IL, which was studied previously by Hall and Lodge.[44] Figure 1a shows the temperature sweep SAOS plots for s-MBsA$_5$ in [C$_2$MIM][TFSI] at a fixed frequency of 1 rad/s in the dark (black symbols) and under UV illumination (red symbols). At 30 °C, the sample is a liquid, with G'' roughly an order of magnitude larger than G', and both moduli initially decrease on heating, which is consistent with heating a well-dissolved polymer solution. However, under both states of illumination, the moduli then begin to increase strongly, with G' exceeding G'' at the ODT temperature. The ordered state G' achieves a value approaching 10 kPa, which is about 3 orders of magnitude larger than the liquid state and becomes independent of temperature with further heating. The ODT is at 92 °C in the dark (black curve), or where AzoMA is in its less soluble *trans* isomer. Upon UV irradiation (red curve), the ODT increases to 120 °C due to the increased solubility of the more polar *cis* isomer.

Figure 1b shows the photoresponsive ODT behavior of a-MBsA$_5$ in [C$_2$MIM][TFSI]. Compared to s-MBsA$_5$ (Figure 1a), the ODT behavior is qualitatively similar (Figure 1b): the ODT in the dark is 89 °C, increasing to 130 °C under UV irradiation. However, the increase in G' with temperature upon ordering is both greater in magnitude and more abrupt than in Figure 1a. This presumably reflects the "cleaner" transition from a liquid state to a lattice of well-defined symmetry, as will be discussed in the structural characterization below.

SAXS experiments were performed to determine the ordered states formed by the various systems above the ODT in the dark. Figure 2 compares the SAXS results for s-MBsA$_5$ and a-MBsA$_5$ at 150 °C. The peak spacings were compared to common block copolymer space group indices, and the pattern for a-MBsA$_5$ (Figure 2b) was readily determined to be hexagonally packed cylinders (HEX), indicated in the figure with dashed vertical lines. The pattern for s-MBsA$_5$ was more difficult to assign. In Figure 2a, the indexing lines present are associated with body-centered-cubic (BCC) spheres. However,

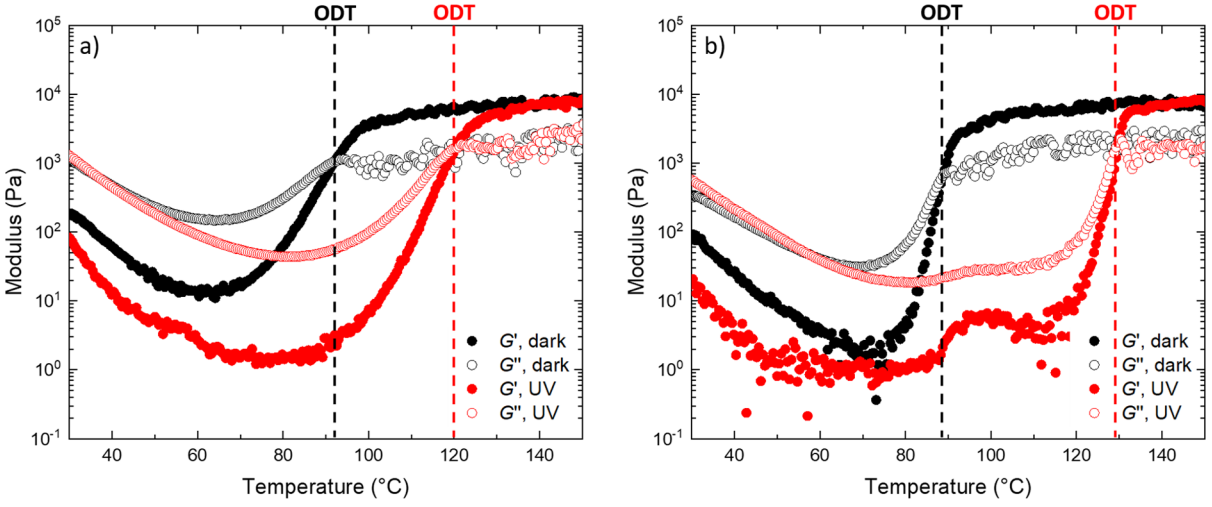

Figure 1. SAOS temperature sweeps for MBsA with 5 mol % incorporation of AzoMA in [C$_2$MIM][TFSI]. The cross-over points, where $G' = G''$, are taken to be the ODTs, are indicated by dashed lines. (a) s-MBsA$_5$, ODT in the dark (black) is 92 °C and under UV (red) is 120 °C. (b) a-MBsA$_5$, ODT in the dark (black) is 89 °C, under UV (red) is 130 °C. Gap: 175 μm, strain 1%, frequency 1 rad/s, temperature ramp 3 °C/min, UV intensity 50 mW/cm^2.

https://doi.org/10.1021/acs.macromol.2c00397
Macromolecules XXXX, XXX, XXX−XXX

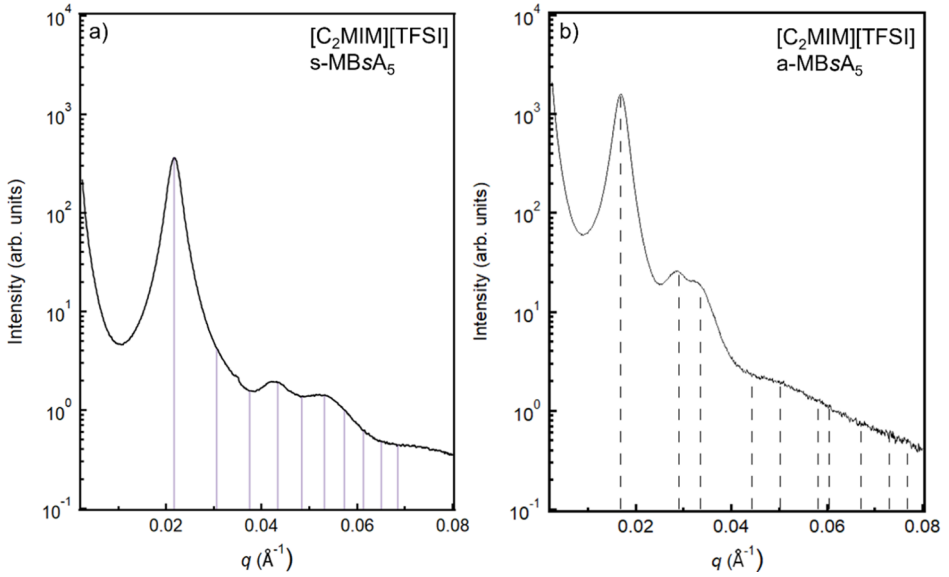

Figure 2. SAXS patterns of (a) s-MB*s*A_5 and (b) a-MB*s*A_5 in [C_2MIM][TFSI] at 150 °C, where the vertical lines are the indexing for particular ordered states. (a) s-MB*s*A_5 does not order into a well-defined pattern and is assigned as a liquid-like packing (LLP) to indicate formation of spheres but no clear lattice, as shown by its non-conformity with BCC spheres (solid lines). (b) Ordered state formed by a-MB*s*A_5 is HEX, as indicated by the dashed indexing lines.

too many peaks are missing from the expected pattern to confidently assign the structure to BCC. The major peaks fit to the pattern 1, square root of 4, and square root of 6, which is not a typical block copolymer pattern. Therefore, for the purposes of this paper, we will refer to this pattern as a liquid-like packing, or LLP, to indicate that the polymers have undergone microphase separation into spherical particles, but that the packing of the spheres is jammed rather than well-ordered onto a lattice.

Returning to photorheology, the significant bistable temperature interval between the ODTs in the dark and under UV presents an opportunity for reversible photo-control of the ODT in both s-MB*s*A_5 and a-MB*s*A_5. This was demonstrated at 100 °C by switching the light filters between 365 nm (UV) and 400−500 nm (vis) in the rheometer. The transition between order and disorder is best revealed by the loss tangent [$\tan(\delta) = G''/G'$], as shown in Figure 3. This triggering was effective almost instantly and was reversible over multiple cycles. The two orders of magnitude change in $\tan(\delta)$ for a-MB*s*A_5 in [C_2MIM][TFSI] indicate that the transitions between the order and disorder permeate through the sample and are not solely located on the interface closest to the UV source.

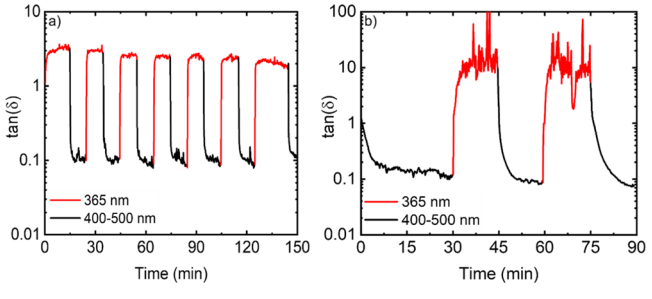

Figure 3. SAOS time sweep for (a) s-MB*s*A_5 in [C_2MIM][TFSI] and (b) a-MB*s*A_5. Temperature was kept constant at 100 °C, and the wavelength of the light source was alternated between 365 nm (red curves) and 400−500 nm (black curves) by changing a light filter. $\tan(\delta) < 1$ indicates order and $\tan(\delta) > 1$ indicates disorder. Transitions are sharp, indicating clean switching between the order and disorder. Gap 175 μm, strain 1%, frequency 1 rad/s, UV intensity 50 mW/cm^2.

Control over the ODT *via* Solvent Selectivity. To enable broader tuning of the phase transition temperature, solvent selectivity was explored. Ueki and Watanabe, Kharel *et al.*, and Carrick *et al.* all showed that the solubility of poly(benzyl methacrylate) in imidazolium [TFSI] ionic liquids can be changed by adjusting the alkyl chain length in the 1-position of the imidazolium group.[51−53] Increasing the chain length decreases the solvent selectivity and therefore increases the LCST of the PBnMA homopolymer. Here, the alkyl chain length was varied from ethyl ([C_2MIM][TFSI]) to methyl ([C_1MIM][TFSI]) and butyl ([C_4MIM][TFSI]). Figure 4a−c compares the linear viscoelastic properties of s-MB*s*A_5 in all three ionic liquids. The ODT decreases to 71 °C in the dark and 88 °C under UV irradiation (Figure 4a) in [C_1MIM]-[TFSI], shifting the bistable ODT window down by 20 °C from its position in [C_2MIM][TFSI] but retaining its width. In the ordered state, G' values remained constant. When the alkyl chain length is increased to [C_4MIM][TFSI], the ODTs increase to above 150 °C, which is beyond the measurement capabilities of the rheometer and therefore can not be detected.

Figure 4d−f depicts the photothermal behavior of a-MB*s*A_5 in all three ionic liquids. A similar trend as with s-MB*s*A_5 is observed, where there is a decrease in the ODT with shorter alkyl tails. The ODT of a-MB*s*A_5 in [C_1MIM][TFSI] in the dark is lower than 30 °C, which is below the temperature range available on the rheometer. However, it has an observable ODT under UV irradiation at 100 °C, suggesting a much wider bistable window. Again, the ODTs are too high to be detected in [C_4MIM][TFSI]. These results suggest that blending pairs of cations in the IL would be a straightforward way to adjust the ODTs continuously across the accessible range.[27,28,39,54−56]

https://doi.org/10.1021/acs.macromol.2c00397
Macromolecules XXXX, XXX, XXX−XXX

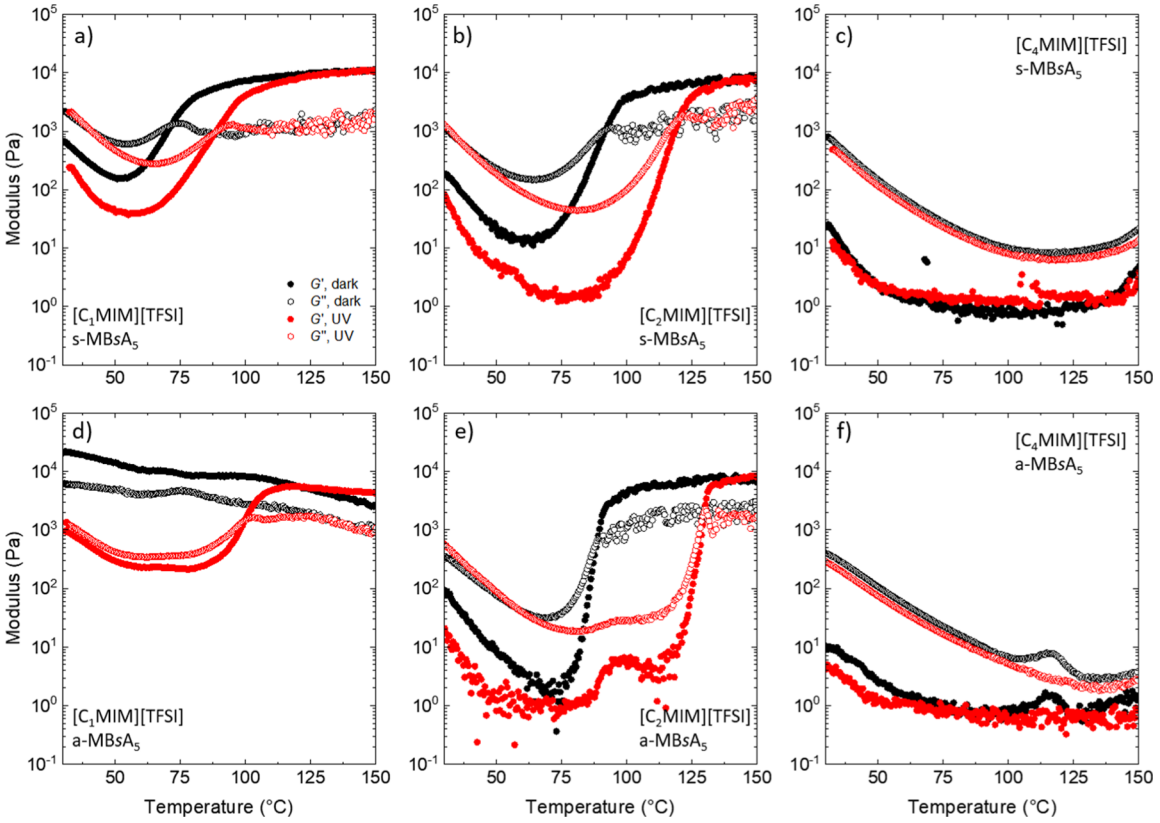

Figure 4. SAOS traces showing the impact of solvent selectivity on ODTs for the MBsA$_5$ polymers in the dark and under UV irradiation. In each figure, black symbols indicate the samples in the dark, while red symbols are under UV irradiation. From left to right, ionic liquids change from [C$_1$MIM][TFSI] to [C$_2$MIM][TFSI] to [C$_4$MIM][TFSI]. (a–c) s-MBsA$_5$ (d–f) a-MBsA$_5$. The ODT increases with increasing IL alkyl chain length for both MBsA polymers, both in the dark and under UV irradiation. Panels (b,d) are the same as in Figure 1a,b, reproduced here for ease of comparison.

All ordered states in the dark were determined by SAXS, and the patterns are shown in Figure 5. For s-MBsA$_5$, the pattern in [C$_1$MIM][TFSI] is the same as in [C$_2$MIM][TFSI], the LLP jammed packing of spheres discussed earlier (Figure 5a,b). The a-MBsA$_5$ samples in the same ionic liquids form HEX (Figure 5d,e). Both polymers in [C$_4$MIM][TFSI] form what might be a complex packing of spheres, such as a Frank–Kasper phase (Figure 5c,f). However, the arrangement of peaks does not correspond clearly to any of the various Frank–Kasper phases observed in block polymers. The peaks can be tentatively assigned to the coexistence of BCC (solid lines in the figure), hexagonally close-packed (HCP, open arrows), and face-centered cubic spheres (FCC, filled arrows).

Control over the ODT *via* AzoMA Content in the Responsive Block. The effect of azobenzene content on the ODT was studied by doubling the AzoMA incorporation in the B block. These changes were made in both the symmetric (s-MBsA$_{12}$, Figure 6a–c) and asymmetric (a-MBsA$_{11}$, Figure 6d–f) cases in all three ionic liquids. Starting with SAOS in [C$_2$MIM][TFSI] (Figure 6b,e), both are already ordered at room temperature in the dark (black symbols), indicating that the increased amount of *trans*--AzoMA further decreases the solubility of the B block. Upon UV irradiation (red symbols), s-MBsA$_{12}$ has G' and G'' overlap from 40 °C until 90 °C, where G' increases to the modulus observed in the dark, indicating a transition to a more defined ordered state (Figure 6b). The structure at intermediate temperatures also appears to reflect a liquid-like packing (Figure S16). a-MBsA$_{11}$ is disordered until 120 °C under UV irradiation, where G' and G'' overlap until 140 °C, where an ordered state is formed (Figure 6e).

For s-MBsA$_{12}$, increasing the solvent selectivity by using [C$_1$MIM][TFSI] resulted in an ordered state at all temperatures, both in the dark and under UV irradiation (Figure 6a). On the other hand, [C$_4$MIM][TFSI] allowed an ODT at 91 °C in the dark and 130 °C under UV irradiation (Figure 6c), which is reminiscent of the behavior of s-MBsA$_5$ in [C$_2$MIM][TFSI]. a-MBsA$_{11}$ shows slightly different behavior. The progression of ODTs in the dark corresponds as expected to the change in solvent selectivity, with the solutions in both [C$_1$MIM][TFSI] (Figure 6d) and [C$_2$MIM][TFSI] (Figure 6e) ordered at all temperatures and in [C$_4$MIM][TFSI] having an ODT at 130 °C (Figure 6f). The behavior under UV irradiation is consistent, with the ODT increasing (albeit relatively weakly) with a change in IL.

Similar to the 5 mol % samples, s-MBsA$_{12}$ and a-MBsA$_{11}$ in [C$_1$MIM][TFSI] and [C$_2$MIM][TFSI] show LLP and HEX patterns in the dark, respectively (Figure 7a,b,d,e). Again in [C$_4$MIM][TFSI], both samples apparently form spheres. s-MBsA$_{12}$ forms a slightly different packing than before, which still does not index clearly onto a well-ordered lattice (Figure 7c). Therefore, it will also be referred to as LLP, even though the packing is apparently slightly different. a-MBsA$_{11}$ forms coexisting HCP (open triangles) and BCC spheres (solid lines) (Figure 7f), similar to the HCP/FCC/BCC seen in the 5 mol % AzoMA system. A summary of the behavior of all samples is found in Table 2.

https://doi.org/10.1021/acs.macromol.2c00397
Macromolecules XXXX, XXX, XXX–XXX

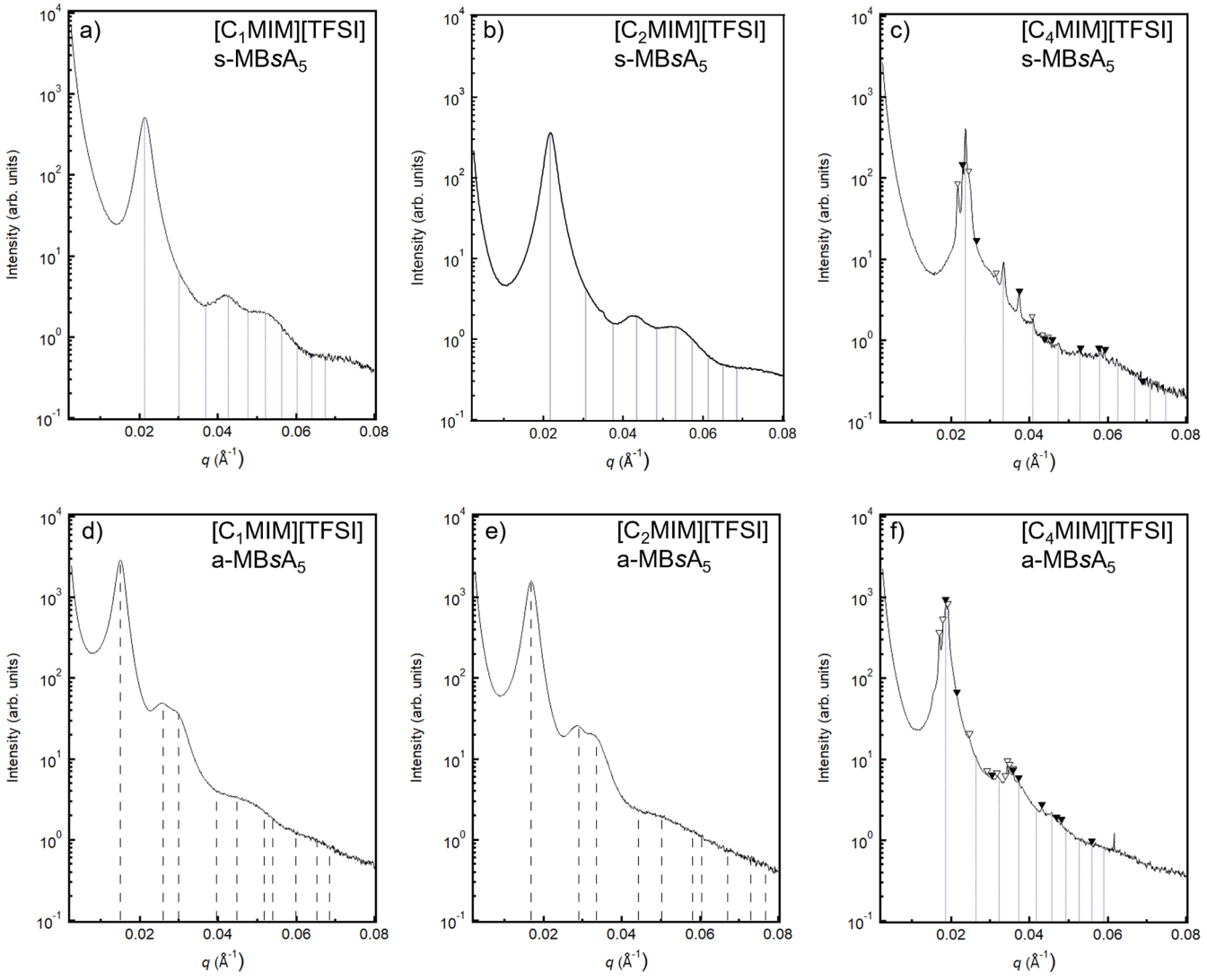

Figure 5. SAXS patterns for s-MBsA$_5$ and a-MBsA$_5$ in all ionic liquids at 150 °C. The lines and symbols indicate indexing for certain ordered states. Black dashed lines are for HEX, solid BCC, open triangles for HCP, and filled triangles for FCC. (a) is s-MBsA$_5$ in [C$_1$MIM][TFSI], ordered to LLP, as demonstrated by the solid indexing lines for BCC not aligning properly. (b) s-MBsA$_5$ in [C$_2$MIM][TFSI], LLP. (c) s-MBsA$_5$ in [C$_4$MIM][TFSI], HCP (open symbols)/FCC (closed symbols)/BCC (solid lines). (d) a-MBsA$_5$ in [C$_1$MIM][TFSI], HEX. (e) a-MBsA$_5$ in [C$_2$MIM][TFSI], HEX. (f) a-MBsA$_5$ in [C$_4$MIM][TFSI], HCP/FCC/BCC.

DISCUSSION

The point of reference for these results is s-MBsA$_5$ in [C$_2$MIM][TFSI]. The ODT temperature window between the sample in the dark and under UV irradiation is 92−120 °C, about 30 °C. Changing the block ratio from 50:50 to 20:80 M/BsA$_5$ has minimal impact on the width of the bistable ODT window. The asymmetric sample, a-MBsA$_5$, has an ODT window from 89 to 130 °C, slightly wider than s-MBsA$_5$. The Flory−Huggins interaction parameter, χ, between the BsA block and the solvent changes with the two isomeric states of the azobenzene. Assuming that the ODT occurs at a fixed χN, N remains constant under the change in irradiation; therefore, the difference in the ODT window is attributable to the dependence of χ on copolymer composition. As UV irradiation is directed from one side of the material, there is the possibility of a change in χ along the thickness of the sample, as UV light is attenuated by the chromophore. Previous work by Hall *et al.* explored the penetration depth of UV light through a statistical copolymer of benzyl methacrylate and 4-phenylazophenyl methacrylate in [C$_2$MIM][TFSI] and found that samples must be thinner than 500 μm to show a difference in phase separation temperatures observed in UV-irradiated samples *versus* those left in the dark.[15] Based on that work, samples in this work were kept thinner than 300 μm. Evidence of penetration through the sample can be seen in the photoswitching rheology (Figure 3) as the UV light causes the sample to clearly disorder, as evidenced by multiple orders of magnitude change in modulus from the ordered state formed under visible irradiation.

From SAXS, the polymers form different ordered states due to their difference in volume fraction of the core block (BsA). Effective volume fractions of the core block ($f_{\mathrm{eff,BsA}}$) can be determined by $f_{\mathrm{eff,M}} = f_{\mathrm{M}}{}^{*}\varphi + (1 - \varphi)$, where f_{M} is the volume fraction of PMMA in the block polymer melt, and φ is the volume fraction of the polymer in ionic liquid. At one extreme, $f_{\mathrm{eff,BsA}} = 1 - f_{\mathrm{eff,M}}$, assuming 100% exclusion of the solvent from the core block.[57] At a constant polymer concentration of 35 wt % in ionic liquid, the $f_{\mathrm{eff,BsA}}$ of s-MBsA is around 0.2 in all ionic liquids and both concentrations of AzoMA and 0.3 for a-

https://doi.org/10.1021/acs.macromol.2c00397
Macromolecules XXXX, XXX, XXX−XXX

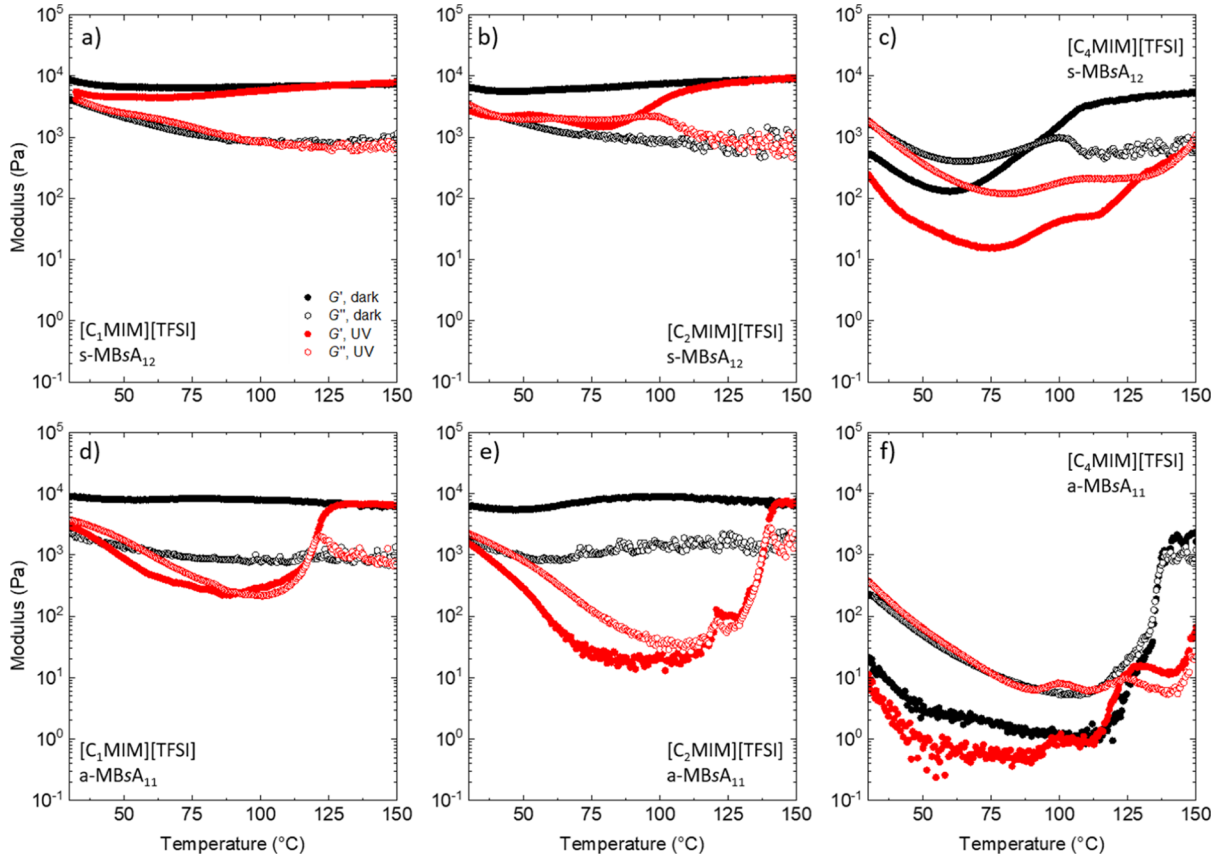

Figure 6. Impact of changing solvent selectivity on ODTs ($G' = G''$) for the MBsA$_{12}$ polymers. Decreasing alkyl chain length decreases the ODT and *vice versa*. In each figure, black symbols indicate the samples in the dark, while red symbols are under UV irradiation. Top row is in [C$_1$MIM][TFSI], middle in [C$_2$MIM][TFSI], and bottom in [C$_4$MIM][TFSI]. (a–c) s-MBsA$_{12}$ (d–f) a-MBsA$_{11}$. ODTs are increasing as the IL alkyl chain length increases.

MBsA. Accordingly, a-MBsA$_5$ forms HEX cylinders (except in [C$_4$MIM][TFSI], discussed below) as expected by the concentration of the core block, while s-MBsA$_5$ forms spheres.

Solvent selectivity in s-MBsA$_5$ has the expected impact: the ODT increases as selectivity decreases. The ODT is lower in [C$_1$MIM][TFSI] than in [C$_2$MIM][TFSI], which is in turn lower than in [C$_4$MIM][TFSI]. For both [C$_1$MIM][TFSI] and [C$_2$MIM][TFSI], the width of the bistable ODT window remains the same, indicating that 5 mol % incorporation of AzoMA undergoing the *trans* to *cis* isomerization causes a similar $\Delta\chi$ in both ionic liquids. In the dark, solvent selectivity contributes to different ordered phases in SAXS. When selectivity is high, in both [C$_1$MIM][TFSI] and [C$_2$MIM]-[TFSI], the ordered state is consistently LLP, whereas in [C$_4$MIM][TFSI], the ordered state is a coexistence of a variety of sphere phases—HCP, FCC, and BCC. The behavior of a-MBsA$_5$ in the same ionic liquids gave a clearer explanation for such behavior. In [C$_1$MIM][TFSI] and [C$_2$MIM][TFSI], the ordered state was HEX, while in [C$_4$MIM][TFSI], it was again HCP/FCC/BCC, indicating that solvent–polymer interactions dominate the behavior rather than block–block interactions, rendering the assumption of 100% exclusion of the solvent from the core inapplicable in this least selective solvent.[57] As rheology indicates that the samples in [C$_4$MIM]-[TFSI] were still disordered at 150 °C, the temperature was increased in SAXS to 175 °C to see if the ordered state resolved to similar packing as in the more selective ionic liquids (Figure S17). s-MBsA$_5$ remained in the BCC/HCP/FCC coexistence state, while a-MBsA$_5$ looks to be evolving toward a HEX state with the HCP peaks merging and new peaks growing in.

Previous work relative to the effect of increasing the concentration of azobenzene on statistical copolymers concerned liquid–liquid phase separation rather than the ODT. Initial studies by Ueki *et al.* found that increasing the AzoMA incorporation from 2 to 4 mol % in BsA statistical copolymers in [C$_2$MIM][TFSI] increased the temperature window between phase separation in the dark and under UV irradiation from 15 to 25 °C.[34] In another study, Ueki *et al.* found that increasing the AzoMA content in statistical copolymers of poly(*N*-isopropylacrylamide) from 8 to 30 mol % increased the temperature window in the UCST from 8 to 50 °C.[58] In contrast, Hall *et al.* found that increasing the AzoMA incorporation in BsA from 6 to 17 mol % did not influence the width of the bistable window, but rather, it decreased the solubility of the polymer in the ionic liquid.[15] Assuming that any change in the ODT window can be attributed to χ, adding more AzoMA should increase $\Delta\chi$, making the window wider. The ODTs for s-MBsA$_{12}$ in [C$_4$MIM][TFSI] are similar to those of s-MBsA$_5$ in [C$_2$MIM]-[TFSI], consistent with Hall *et al.*'s results. s-MBsA$_{12}$ is also the only sample in [C$_4$MIM][TFSI] that did not form coexisting BCC/FCC/HCP, suggesting that, for the symmetric case, increasing the AzoMA concentration effectively increases the solvent selectivity. However, the asymmetric samples align more with Ueki *et al.*'s results, especially in the case of

https://doi.org/10.1021/acs.macromol.2c00397
Macromolecules XXXX, XXX, XXX–XXX

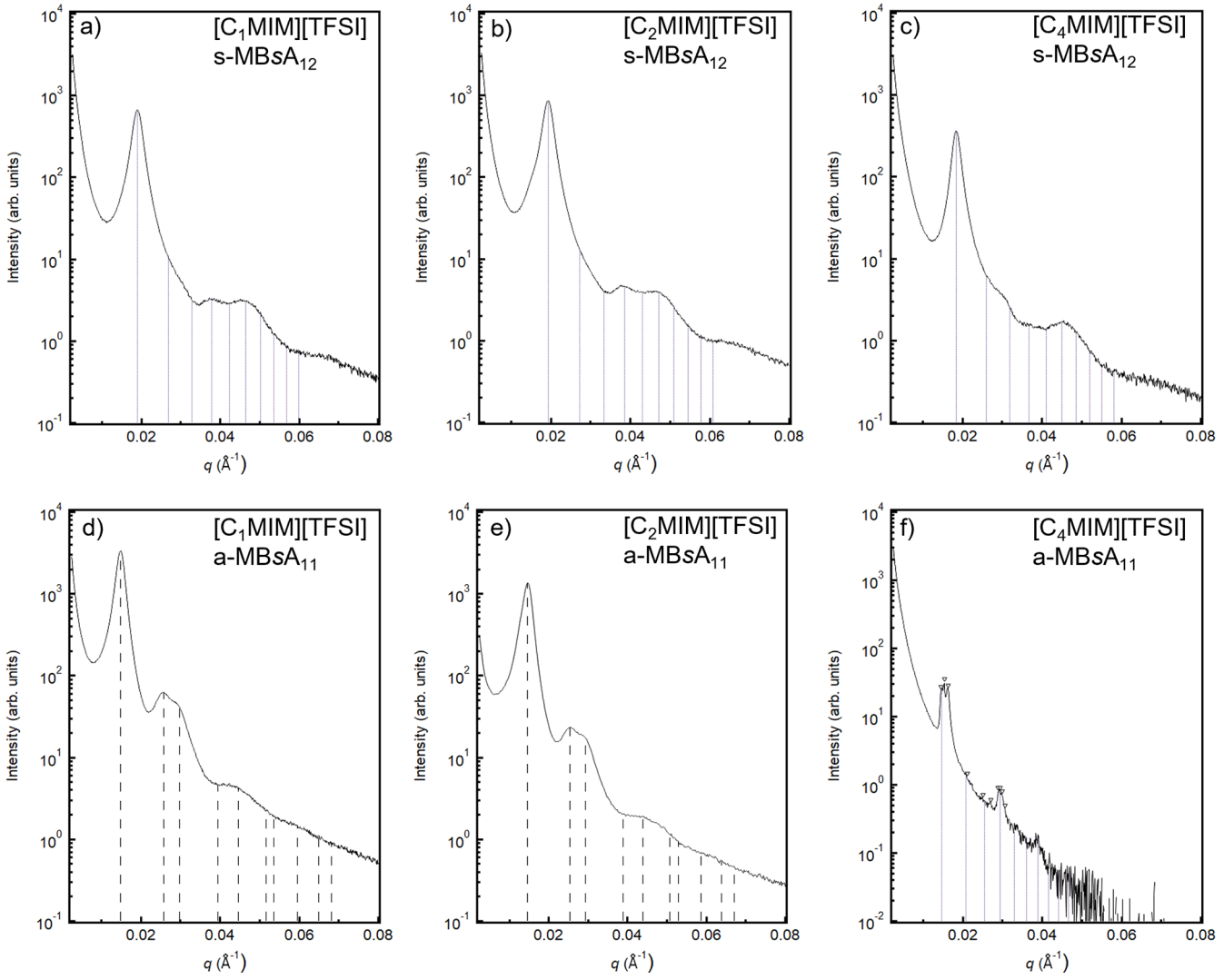

Figure 7. SAXS patterns for s-MBsA$_{12}$ and a-MBsA$_{11}$ in all ionic liquids at 150 °C. The lines and symbols indicate indexing for certain ordered states. Dashed lines are for HEX, solid lines for BCC, open triangles for HCP, and filled triangles for FCC. (a) s-MBsA$_{12}$ in [C$_1$MIM][TFSI], assigned as LLP. (b) s-MBsA$_{12}$ in [C$_2$MIM][TFSI], LLP. (c) s-MBsA$_{12}$ in [C$_4$MIM][TFSI], LLP. (d) a-MBsA$_{11}$ in [C$_1$MIM][TFSI], HEX. (e) a-MBsA$_{11}$ in [C$_2$MIM][TFSI], HEX. (f) a-MBsA$_{11}$ in [C$_4$MIM][TFSI], HCP/BCC.

Table 2. Summary of ODTs

				ODT (°C)		
Polymer	n_{AzoMA} (mol %)	f_{PMMA}	Irradiation	[C$_1$MIM][TFSI]	[C$_2$MIM][TFSI]	[C$_4$MIM][TFSI]
s-MBsA$_5$	5	0.5	dark	71	92	disordered
			UV	88	120	disordered
a-MBsA$_5$	5	0.2	dark	ordered	89	disordered
			UV	100	130	disordered
s-MBsA$_{12}$	12	0.5	dark	ordered	ordered	91
			UV	ordered	42−90	130
a-MBsA$_{11}$	11	0.3	dark	ordered	ordered	132
			UV	92−120	120−140	137

[C$_2$MIM][TFSI]. For a-MBsA$_{11}$, the dark ODT is below 30 °C, while under UV irradiation is 130 °C, in comparison to the 89−130 °C window for a-MBsA$_5$. Further studies are necessary to fully explore and understand the connection between the AzoMA isomer solubility change and solvent selectivity changes with alkyl chain length modification in imidazolium-based ionic liquids.

CONCLUSIONS

This work focused on characterizing the ODTs of thermo- and photoresponsive block copolymer solutions with varying block ratios, solvent selectivity, and photoactive monomer content. Varying the less soluble block content from symmetric to asymmetric with a 5 mol % Azo monomer in [C$_2$MIM][TFSI] did not have a large impact on the ODT of the system but rather accessed the HEX instead of the LLP ordered state.

https://doi.org/10.1021/acs.macromol.2c00397
Macromolecules XXXX, XXX, XXX−XXX

Adjusting the solvent selectivity was the most convenient method for adjusting the ODT temperature, especially in the s-MBsA system. As the alkyl chain length of the IL increased, the ODT moved to higher temperatures. In general, the asymmetric polymer samples had slightly higher ODTs under UV irradiation than the symmetric samples. Increasing the azobenzene content of the responsive block caused the ODT to decrease in the dark due to the insolubility of *trans* azobenzene.

■ ASSOCIATED CONTENT

Supporting Information

The Supporting Information is available free of charge at https://pubs.acs.org/doi/10.1021/acs.macromol.2c00397.

Proton and fluorine nuclear magnetic resonance spectra, size exclusion chromatographs for polymer and ionic liquid characterization, and SAXS patterns for intermediate temperatures for s-MBsA$_{12}$ and at high temperature for s-MBsA$_5$ and a-MBsA$_5$ in [C$_4$MIM][TFSI] (PDF)

■ AUTHOR INFORMATION

Corresponding Author

Timothy P. Lodge − *Department of Chemistry and Department of Chemical Engineering and Materials Science, University of Minnesota, Minneapolis, Minnesota 55455, United States;* orcid.org/0000-0001-5916-8834; Email: lodge@umn.edu

Authors

Claire L. Seitzinger − *Department of Chemistry, University of Minnesota, Minneapolis, Minnesota 55455, United States*

Cecilia C. Hall − *Department of Chemistry, University of Minnesota, Minneapolis, Minnesota 55455, United States;* orcid.org/0000-0003-2773-1279

Complete contact information is available at: https://pubs.acs.org/10.1021/acs.macromol.2c00397

Notes

The authors declare no competing financial interest.

■ ACKNOWLEDGMENTS

This work was supported through the NSF Polymers Program DMR-1797578 and DMR-2103630. The SAXS measurements were performed at the DuPont-Northwestern-Dow Collaborative Access Team (DND-CAT) located at Sector 5 of the Advanced Photon Source (APS). DND-CAT is supported by E.I. DuPont de Nemours & Co., the Dow Chemical Company, and Northwestern University. Use of the APS, an Office of Science User Facility operated for the U.S. DOE Office of Science by Argonne National Laboratory, was supported by the U.S. DOE under contract no. DE-AC02-06CH11357. We would like to thank S. Piril Ertem for editing, David Giles for discussions about the rheology, and Aaron Lindsay and Andreas Mueller for writing and refining an Igor code for indexing SAXS patterns (https://doi.org/10.13020/9m8p-pv93).

■ REFERENCES

(1) Ye, Y.-S.; Rick, J.; Hwang, B.-J. Ionic Liquid Polymer Electrolytes. *J. Mater. Chem. A* **2013**, *1*, 2719−2743.

(2) Kelly, J. C.; Degrood, N. L.; Roberts, M. E. Li-Ion Battery Shut-off at High Temperature Caused by Polymer Phase Separation in Responsive Electrolytes. *Chem. Commun.* **2015**, *51*, 5448−5451.

(3) Thelen, J. L.; Wang, A. A.; Chen, X. C.; Jiang, X.; Schaible, E.; Balsara, N. P. Correlations between Salt-Induced Crystallization, Morphology, Segmental Dynamics, and Conductivity in Amorphous Block Copolymer Electrolytes. *Macromolecules* **2018**, *51*, 1733−1740.

(4) Wakayama, H.; Yonekura, H.; Kawai, Y. Three-Dimensional Bicontinuous Nanocomposite from a Self-Assembled Block Copolymer for a High-Capacity All-Solid-State Lithium Battery Cathode. *Chem. Mater.* **2016**, *28*, 4453−4459.

(5) Liu, S.; Zhou, L.; Wang, P.; Zhang, F.; Yu, S.; Shao, Z.; Yi, B. Ionic-Liquid-Based Proton Conducting Membranes for Anhydrous H2/Cl2 Fuel-Cell Applications. *ACS Appl. Mater. Interfaces* **2014**, *6*, 3195−3200.

(6) Park, M. J.; Choi, I.; Hong, J.; Kim, O. Polymer Electrolytes Integrated with Ionic Liquids for Future Electrochemical Devices. *J. Appl. Polym. Sci.* **2013**, *129*, 2363−2376.

(7) Saba, S. A.; Mousavi, M. P. S.; Bühlmann, P.; Hillmyer, M. A. Hierarchically Porous Polymer Monoliths by Combining Controlled Macro- and Microphase Separation. *J. Am. Chem. Soc.* **2015**, *137*, 8896−8899.

(8) Chen, L.; Phillip, W. A.; Cussler, E. L.; Hillmyer, M. A. Robust Nanoporous Membranes Templated by a Doubly Reactive Block Copolymer. *J. Am. Chem. Soc.* **2007**, *129*, 13786−13787.

(9) Jackson, E. A.; Lee, Y.; Hillmyer, M. A. ABAC Tetrablock Terpolymers for Tough Nanoporous Filtration Membranes. *Macromolecules* **2013**, *46*, 1484−1491.

(10) Phillip, W. A.; Amendt, M.; O'Neill, B.; Chen, L.; Hillmyer, M. A.; Cussler, E. L. Diffusion and Flow across Nanoporous Polydicyclopentadiene-Based Membranes. *ACS Appl. Mater. Interfaces* **2009**, *1*, 472−480.

(11) Preman, N. K.; Barki, R. R.; Vijayan, A.; Sanjeeva, S. G.; Johnson, R. P. Recent Developments in Stimuli-Responsive Polymer Nanogels for Drug Delivery and Diagnostics: A Review. *Eur. J. Pharm. Biopharm.* **2020**, *157*, 121−153.

(12) Zhang, Q.; Zhang, Y.; Wan, Y.; Carvalho, W.; Hu, L.; Serpe, M. J. Stimuli-Responsive Polymers for Sensing and Reacting to Environmental Conditions. *Prog. Polym. Sci.* **2021**, *116*, 101386.

(13) Gately, T. J.; Li, W.; Mostafavi, S. H.; Bardeen, C. J. Reversible Adhesion Switching Using Spiropyran Photoisomerization in a High Glass Transition Temperature Polymer. *Macromolecules* **2021**, *54*, 9319−9326.

(14) Bütün, V.; Billingham, N. C.; Armes, S. P. Unusual Aggregation Behavior of a Novel Tertiary Amine Methacrylate-Based Diblock Copolymer: Formation of Micelles and Reverse Micelles in Aqueous Solution. *J. Am. Chem. Soc.* **1998**, *120*, 11818−11819.

(15) Hall, C. C.; Rivera, C. A.; Lodge, T. P. The Effect of Light Penetration Depth on the LCST Phase Behavior of a Thermo- and Photoresponsive Statistical Copolymer in an Ionic Liquid. *J. Polym. Sci., Part A: Polym. Chem.* **2019**, *57*, 281−287.

(16) Ueki, T.; Nakamura, Y.; Usui, R.; Kitazawa, Y.; So, S.; Lodge, T. P.; Watanabe, M. Photoreversible Gelation of a Triblock Copolymer in an Ionic Liquid. *Angew. Chem., Int. Ed.* **2015**, *54*, 3018−3022.

(17) Lee, H.-N.; Newell, N.; Bai, Z.; Lodge, T. P. Unusual Lower Critical Solution Temperature Phase Behavior of Poly(Ethylene Oxide) in Ionic Liquids. *Macromolecules* **2012**, *45*, 3627−3633.

(18) Lachwa, J.; Szydlowski, J.; Najdanovic-Visak, V.; Rebelo, L. P. N.; Seddon, K. R.; Nunes da Ponte, M.; Esperança, J. M. S. S.; Guedes, H. J. R. Evidence for Lower Critical Solution Behavior in Ionic Liquid Solutions. *J. Am. Chem. Soc.* **2005**, *127*, 6542−6543.

(19) Dudowicz, J.; Freed, K. F. Explanation for the Unusual Phase Behavior of Polystyrene-b-Poly(*n*-Alkyl Methacrylate) Diblock Copolymers: Specific Interactions. *Macromolecules* **2000**, *33*, 5292−5299.

(20) Russell, T. P.; Karis, T. E.; Gallot, Y.; Mayes, A. M. A Lower Critical Ordering Transition in a Diblock Copolymer Melt. *Nature* **1994**, *368*, 729−731.

(21) Ryu, D. Y.; Jeong, U.; Kim, J. K.; Russell, T. P. Closed-Loop Phase Behaviour in Block Copolymers. *Nat. Mater.* **2002**, *1*, 114−117.
(22) Ruzette, A.-V. G.; Banerjee, P.; Mayes, A. M.; Pollard, M.; Russell, T. P.; Jerome, R.; Slawecki, T.; Hjelm, R.; Thiyagarajan, P. Phase Behavior of Diblock Copolymers between Styrene and *n*-Alkyl Methacrylates. *Macromolecules* **1998**, *31*, 8509−8516.
(23) Ueki, T. Stimuli-Responsive Polymers in Ionic Liquids. *Polym. J.* **2014**, *46*, 646−655.
(24) Halperin, A.; Kröger, M.; Winnik, F. M. Poly(*N*-isopropylacrylamide) Phase Diagrams: Fifty Years of Research. *Angew. Chem., Int. Ed.* **2015**, *54*, 15342−15367.
(25) Kujawa, P.; Winnik, F. M. Volumetric Studies of Aqueous Polymer Solutions Using Pressure Perturbation Calorimetry: A New Look at the Temperature-Induced Phase Transition of Poly(*N*-Isopropylacrylamide) in Water and D_2O. *Macromolecules* **2001**, *34*, 4130−4135.
(26) Heskins, M.; Guillet, J. E. Solution Properties of Poly(N-Isopropylacrylamide). *J. Macromol. Sci., Part A: Pure Appl.Chem.* **1968**, *2*, 1441−1455.
(27) Lee, H.-N.; Lodge, T. P. Poly(*n*-butyl methacrylate) in Ionic Liquids with Tunable Lower Critical Solution Temperatures (LCST). *J. Phys. Chem. B* **2011**, *115*, 1971−1977.
(28) Hoarfrost, M. L.; He, Y.; Lodge, T. P. Lower Critical Solution Temperature Phase Behavior of Poly(*n*-butyl methacrylate) in Ionic Liquid Mixtures. *Macromolecules* **2013**, *46*, 9464−9472.
(29) Ueki, T.; Arai, A. A.; Kodama, K.; Kaino, S.; Takada, N.; Morita, T.; Nishikawa, K.; Watanabe, M. Thermodynamic study on phase transitions of poly(benzyl methacrylate) in ionic liquid solvents. *Pure Appl. Chem.* **2009**, *81*, 1829−1841.
(30) Fujii, K.; Ueki, T.; Niitsuma, K.; Matsunaga, T.; Watanabe, M.; Shibayama, M. Structural aspects of the LCST phase behavior of poly(benzyl methacrylate) in room-temperature ionic liquid. *Polymer* **2011**, *52*, 1589−1595.
(31) Kobayashi, Y.; Kitazawa, Y.; Hashimoto, K.; Ueki, T.; Kokubo, H.; Watanabe, M. Thermosensitive phase separation behavior of poly(benzyl methacrylate)/solvate ionic liquid solutions. *Langmuir* **2017**, *33*, 14105−14114.
(32) Fujii, K.; Ueki, T.; Hashimoto, K.; Kobayashi, Y.; Kitazawa, Y.; Hirosawa, K.; Matsugami, M.; Ohara, K.; Watanabe, M.; Shibayama, M. Microscopic structure of solvated poly(benzyl methacrylate) in an imidazolium-based ionic liquid: high-energy X-ray total scattering and all-atom MD simulation study. *Macromoecules* **2017**, *50*, 4780−4786.
(33) Hirosawa, K.; Fujii, K.; Ueki, T.; Kitazawa, Y.; Littrell, K. C.; Watanabe, M.; Shibayama, M. SANS study on the solvated structure and molecular interactions of a thermo-responsive polymer in a room temperature ionic liquid. *Phys. Chem. Chem. Phys.* **2016**, *18*, 17881−17889.
(34) Ueki, T.; Yamaguchi, A.; Ito, N.; Kodama, K.; Sakamoto, J.; Ueno, K.; Kokubo, H.; Watanabe, M. Photoisomerization-Induced Tunable LCST Phase Separation of Azobenzene-Containing Polymers in an Ionic Liquid. *Langmuir* **2009**, *25*, 8845−8848.
(35) Ueki, T.; Usui, R.; Kitazawa, Y.; Lodge, T. P.; Watanabe, M. Thermally Reversible Ion Gels with Photohealing Properties Based on Triblock Copolymer Self-Assembly. *Macromolecules* **2015**, *48*, 5928−5933.
(36) Ueki, T.; Yamaguchi, A.; Watanabe, M. Unlocking of Interlocked Heteropolymer Gel by Light: Photoinduced Volume Phase Transition in an Ionic Liquid from a Metastable State to an Equilibrium Phase. *Chem. Commun.* **2012**, *48*, 5133.
(37) Ye, Q.; Huo, M.; Zeng, M.; Liu, L.; Peng, L.; Wang, X.; Yuan, J. Photoinduced Reversible Worm-to-Vesicle Transformation of Azo-Containing Block Copolymer Assemblies Prepared by Polymerization-Induced Self-Assembly. *Macromolecules* **2018**, *51*, 3308−3314.
(38) Zhao, D.; Ma, Y.; Lodge, T. P. Exchange Kinetics for a Single Block Copolymer in Micelles of Two Different Sizes. *Macromolecules* **2018**, *51*, 2312−2320.
(39) Wang, C.; Ma, X.; Kitazawa, Y.; Kobayashi, Y.; Zhang, S.; Kokubo, H.; Watanabe, M. From Macromolecular to Small-Molecular Triggers: Facile Method toward Photoinduced LCST Phase Behavior of Thermoresponsive Polymers in Mixed Ionic Liquids Containing an Azobenzene Moiety. *Macromol. Rapid Commun.* **2016**, *37*, 1960−1965.
(40) Wang, C.; Dong, W.; Li, P.; Wang, Y.; Tu, H.; Tan, S.; Wu, Y.; Watanabe, M. Reversible Ion-Conducting Switch by Azobenzene Molecule with Light-Controlled Sol−Gel Transitions of the PNIPAm Ion Gel. *ACS Appl. Mater. Interfaces* **2020**, *12*, 42202−42209.
(41) Lan, X.; Ma, X.; Wang, L.; Shi, Y.; Gu, Q.; Wu, L.; Gu, X.; Luo, Z. Self-Assembly of Diblock Copolymers Containing Thermo- and Photoresponsive Lower Critical Solution Temperature Phase Behavior Polymer with Tunable Assembly Temperature in an Ionic Liquid Mixture. *ACS Omega* **2019**, *4*, 11229−11236.
(42) Hartley, G. S. The Cis-Form of Azobenzene. *Nature* **1937**, *140*, 281.
(43) Bullock, D. J. W.; Cumper, C. W. N.; Vogel, A. I. 989. Physical Properties and Chemical Constitution. Part XLIII. The Electric Dipole Moments of Azobenzene, Azopyridines, and Azoquinolines. *J. Chem. Soc.* **1965**, 5316.
(44) Hall, C. C.; Lodge, T. P. Photoreversible Order−Disorder Transition in an Ionic Liquid Solvated Block Polymer. *ACS Macro Lett.* **2019**, *8*, 393−398.
(45) Shimoboji, T.; Ding, Z.; Stayton, P. S.; Hoffman, A. S. Mechanistic Investigation of Smart Polymer−Protein Conjugates. *Bioconjugate Chem.* **2001**, *12*, 314−319.
(46) Lundin, F.; Hansen, H. W.; Adrjanowicz, K.; Frick, B.; Rauber, D.; Hempelmann, R.; Shebanova, O.; Niss, K.; Matic, A. Pressure and Temperature Dependence of Local Structure and Dynamics in an Ionic Liquid. *J. Phys. Chem. B* **2021**, *125*, 2719−2728.
(47) Chemical Retrieval on the Web. Polymer Properties Database. https://polymerdatabase.com/home.html.
(48) Jackson, C.; Chen, Y.-J.; Mays, J. W. Size Exclusion Chromatography with Multiple Detectors: Solution Properties of Linear Chains of Varying Flexibility in Tetrahydrofuran. *J. Appl. Polym. Sci.* **1996**, *61*, 865−874.
(49) Podzimek, S. *Light Scattering, Size Exclusion Chromatography and Asymmetric Flow Field Flow Fractionation*; John Wiley & Sons, Inc.: Hoboken, NJ, USA, 2011.
(50) Tuzar, Z.; Kratochvíl, P. Determination of the Composition of Copolymers by Differential Refractometry in Mixed Solvents. *Polym. Lett.* **1969**, *7*, 825−828.
(51) Ueki, T.; Watanabe, M. Lower Critical Solution Temperature Behavior of Linear Polymers in Ionic Liquids and the Corresponding Volume Phase Transition of Polymer Gels. *Langmuir* **2007**, *23*, 988−990.
(52) Kharel, A.; Hall, C.; Černoch, P.; Stepanek, P.; Lodge, T. P. Dilute Solution Properties of Poly(Benzyl Methacrylate) in Ionic Liquids. *Macromolecules* **2020**, *53*, 885−894.
(53) Carrick, B. R.; Seitzinger, C. L.; Lodge, T. P. Unusual Lower Critical Solution Temperature Phase Behavior of Poly(Benzyl Methacrylate) in a Pyrrolidinium-Based Ionic Liquid. *Molecules* **2021**, *26*, 4850.
(54) Lee, H.-N.; Lodge, T. P. Lower Critical Solution Temperature (LCST) Phase Behavior of Poly(Ethylene Oxide) in Ionic Liquids. *J. Phys. Chem. Lett.* **2010**, *1*, 1962−1966.
(55) Lee, H.-N.; Bai, Z.; Newell, N.; Lodge, T. P. Micelle/Inverse Micelle Self-Assembly of a PEO−PNIPAm Block Copolymer in Ionic Liquids with Double Thermoresponsivity. *Macromolecules* **2010**, *43*, 9522−9528.
(56) Kodama, K.; Nanashima, H.; Ueki, T.; Kokubo, H.; Watanabe, M. Lower Critical Solution Temperature Phase Behavior of Linear Polymers in Imidazolium-Based Ionic Liquids: Effects of Structural Modifications. *Langmuir* **2009**, *25*, 3820−3824.
(57) Hanley, K. J.; Lodge, T. P.; Huang, C.-I. Phase Behavior of a Block Copolymer in Solvents of Varying Selectivity. *Macromolecules* **2000**, *33*, 5918−5931.
(58) Ueki, T.; Nakamura, Y.; Yamaguchi, A.; Niitsuma, K.; Lodge, T. P.; Watanabe, M. UCST Phase Transition of Azobenzene-Containing Random Copolymer in an Ionic Liquid. *Macromolecules* **2011**, *44*, 6908−6914.

https://doi.org/10.1021/acs.macromol.2c00397
Macromolecules XXXX, XXX, XXX−XXX